Multifractal Conductance Fluctuations of Helical Edge States

E. B. Olshanetsky,[1,2] G. M. Gusev,[3] A. D. Levin,[3] Z. D. Kvon,[1,2] and N. N. Mikhailov[1,2]
[1]Institute of Semiconductor Physics, Novosibirsk 630090, Russia
[2]Novosibirsk State University, Novosibirsk 630090, Russia
[3]Instituto de Física da Universidade de São Paulo, 135960-170 São Paulo, SP, Brazil

(Received 10 March 2023; accepted 23 July 2023; published 16 August 2023)

Two-dimensional topological insulators are characterized by the bulk gap and one-dimensional helical states running along the edges. The theory predicts the topological protection of the helical transport from coherent backscattering. However, the unexpected deviations of the conductance from the quantized value and localization of the helical modes are generally observed in long samples. Moreover, at millikelvin temperatures significant mesoscopic fluctuations are developed as a function of the electron energy. Here we report the results of an experimental study of the transport in a HgTe quantum well with an inverted energy spectrum that reveal a multifractality of the conductance fluctuations in the helical edge state dominated transport regime. We attribute observed multifractality to mesoscopic fluctuations of the electron wave function or local density of states at the spin quantum Hall transition. We have shown that the mesoscopic two-dimensional topological insulator provides a highly tunable experimental system in which to explore the physics of the Anderson transition between topological states.

DOI: 10.1103/PhysRevLett.131.076301

The theory predicts the existence of a special class of solid state materials characterized by an energy gap for the electron bulk states and gapless helical edge states with a rigid spin-momentum coupling [1–4]. In the absence of interaction the helical edge transport is topologically protected due to the time-reversal symmetry (TRS) so that the sample conductance is expected to be quantized in the units of $G_0 = 2e^2/h$. In reality these predicted universal conductance values are found only in samples with short edge channel lengths [5–7]. The unexpected elastic backscattering between helical edge states present in a two-dimensional topological insulators (2D TI) is the subject of numerous debates and remains a long-standing hot topic [8–10]. Some of the more popular models proposed to explain the suppression of ballistic conductance consider mechanisms that break the TRS, such as magnetic impurities and nuclear spin [11–14]. While other models take into account mechanisms that do not violate the TRS, such as weakly interacting generic helical liquid and generic helical Tomonaga-Luttinger liquid [15,16], noise-induced backscattering [17], phonons [18], random spin-orbit interaction [19]. Since the two-dimensional topological insulators generally have a small bulk energy gap, the random potential created by impurities may result in the formation of charge puddles or quantum dots with spin-degenerate states [20,21]. Thus, when the Fermi energy of the helical channel is aligned with one of the dot-puddle levels, the electron can tunnel into the puddle, interact with another electron, and get scattered back.

Different theoretical models predict different conductance dependencies on temperature, length, and gate voltage bias and can, therefore, be experimentally differentiated. In most experimental observations the helical edges' conductance, even for $G \ll G_0$ [7,22–24], has only a very weak T dependence or no T dependence at all. This result disagrees with the majority of models that predict a suppression of correction to conductance in the low-temperature limit. Another observation contradicting the theoretical expectations is the reproducible mesoscopic fluctuations of both the local and nonlocal resistance as a function of gate voltage, which have been observed in HgTe quantum wells (QW) at millikelvin temperatures [7,25].

Several mechanisms have been proposed for the explanation of the low-temperature quasiperiodic fluctuations. The first one involves quantum interference of the elastically scattered electronic waves in a disordered system. Note, however, that most of the TRS-neutral perturbations, considered above, involve inelastic processes, and, therefore, would suppress quantum interference. Recently it has been shown that an ensemble of magnetic impurities may cause time-reversal symmetry-preserving quasielastic backscattering, leading to mesoscopic fluctuations of the helical edge conductance [26]. However, the magnetic contamination is unlikely to occur during the MBE growth of clean materials.

Secondly, mesoscopic fluctuations with gate voltage can be attributed to the random potential created by charged impurities, resulting in the formation of puddles in a narrow gap material. Near a long edge, there can be multiple puddles, and backscattering occurs when the Fermi energy aligns with a level in one of them [20].

Third, mesoscopic fluctuations could be due to the local density of the state fluctuations and related to Anderson localization transition [27].

In the present Letter we analyze the scaling behavior of the mesoscopic conductance fluctuations (MCF) in HgTe wells whith the helical edge transport and observe multifractality of the MCF as a function of the gate voltage. Multifractal structures of fluctuations are characterized by an infinite set of critical scaling exponents of the power law of the probability density. Multifractal analysis is a useful method to investigate various properties in many fields that has recently received more attention by scientists due to its ability to describe complexity and irregularity of the system behavior. In condensed matter physics signatures of multifractality appear in Anderson transitions [27], quantum Hall effect [28,29], at the spin quantum Hall transition [28,30], superconductor-insulator transition in disordered films [31], and disorder-induced multifractal superconductivity [32]. The direct experimental measurement of multifractality is a challenging task. The remarkable example is the universal conductance fluctuations due to quantum interference effects caused by multiple wave scattering inside a sample [33]. Recently multifractality in the conductance fluctuations versus magnetic field has been detected in a single layer graphene sample near the Dirac point [34]. This multifractality has been attributed to the Anderson localization near the Dirac point. However, a one-to-one correspondence between the multifractality of a electronic wave function and the multifractality of MCF must be justified. In Ref. [35] it has been argued that the multifractality in graphene is the effect of magnetic field induced trajectory correlations in a specific stochastic process.

Recently it has been shown that conductance fluctuations display multifractality in the integer quantum Hall plateau-to-plateau transitions in high-mobility mesoscopic graphene devices [36]. The multifractal complex hierarchical phenomena in quantum Hall effect is expected, when the edge states penetrate into the bulk and a complex spatial pattern develops, leading to the formation of coherent structures of different sizes inside the sample [29].

Therefore, multifractal analysis can be used as an important method for the characterization and description of complex hierarchical chaotic phenomena. Note that the scaling behavior of conductance fluctuation as a function of the Fermi energy has not been studied yet.

We have measured the resistance of the quantum wells $Cd_{0.65}Hg_{0.35}Te/HgTe/Cd_{0.65}Hg_{0.35}Te$ with (013) (devices B, C) and (001)(device A) surface orientations and the well thickness of 8.3–8.5 nm [37]. Layer sequence scheme and details of the sample preparation have been published previously [38]. Devices for study are mesoscopic Hall bars with 9 voltage probes and the width W of 3 μm separated into 3 segments of different length L $(3, 8, 33$ μm) between

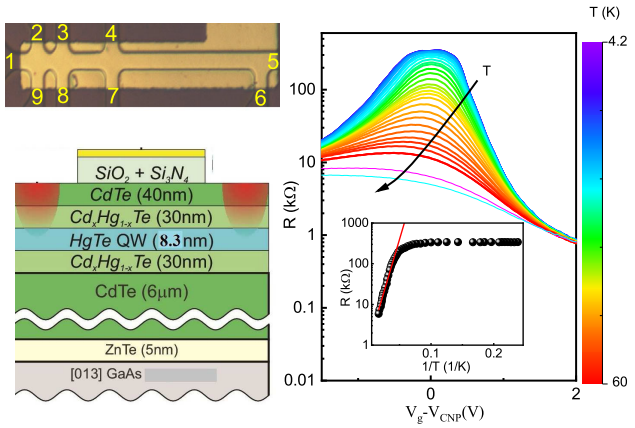

FIG. 1. Left: schematic of the transistor and the top view of the sample. Right: resistance $R^{1,5}_{7,6}(V_g)$ as a function of gate voltage measured at different temperatures. Insert: resistance at the CNP $(V_g - V_{\mathrm{CNP}} = 0)$ as a function of $1/\mathrm{T}$. Solid red line corresponds to $R \sim \exp(\Delta/2kT)$ with $\Delta = 20$ meV.

the probes. The top panel in Fig. 1 shows the device layout and the numbering of the probes. The measurements of the resistance $R(T)$ have been performed in the temperature range 80 mK–1 K. The measurement details are presented in the Supplemental Material [37].

Prior to focusing on the low-temperature transport characteristics we examine the properties at high T. Figure 1 shows the variation of the resistance with gate voltage in the temperature range $4.2 < T < 60$ K. The resistance around the charge neutrality point (CNP) decreases exponentially for temperatures above 15 K while saturating below 10 K. The profile of the resistance temperature dependencies above $T > 15$ K follows the activation law $R(T) \sim \exp(\Delta/2kT)$, where Δ is the activation gap. Therefore the thermally activated behavior of conductance above 15 K corresponds to a gap of 20 meV between the conduction and valence bands in the HgTe well. Below 10 K near CNP we observe the helical edge state dominated transport. Note, however, that the maximum resistance strongly exceeds the $h/2e^2$ value predicted for the helical transport with the TRS intact. As mentioned in the Introduction, edge state electron scattering to multiple puddles can be responsible for the large edge states' resistance. Owing to the presence of random potential, the conduction and valence bands exhibit Gaussian tails that extend into the band gap. According to the localization theory, electrons and holes residing in these band tails should be localized. The observation of nonlocal resistance supports this notion, indicating that transport within the gap is facilitated by the helical states [10]. To ensure coverage of the mobility gap in our devices, at low temperatures we employed an interval of approximately 1 volt near CNP.

Now we focus on the helical edge state dominated transport at low temperatures. Figure 2(a) shows the conductance $G(V_g) = 1/R^{3,4}_{3,4}$ as a function of gate voltage

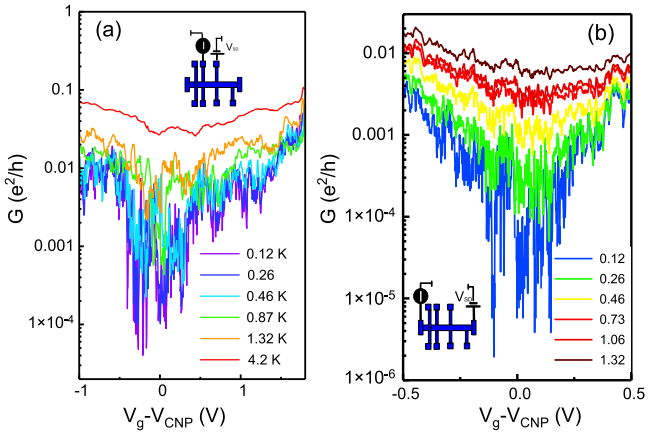

FIG. 2. Conductance as a function of the gate voltage at different temperatures for sample A for different voltage probes. (a) $G(V_g) = 1/R^{3,4}_{3,4}$. (b) $G(V_g) = 1/R^{1,5}_{1,5}$.

and temperature in the units of e^2/h measured by using the two probe voltage source scheme because of the large resistance value. The conductance is found to be much lower than the e^2/h quantum and to exhibit relatively large reproducible fluctuations at low temperatures (for details see the Supplemental Material [37]). The conductance fluctuations persist up to temperatures as high as 4.2 K. It is evident that the oscillations exhibit a distinctive feature of fractality, characterized by large amplitudes and wide frequency variations. We have also measured the conductance fluctuations for different probes. Figure 2(b) shows the evolution of the conductance with temperature measured for a long device segment: $G(V_g) = 1/R^{1,5}_{1,5}$. Reproducible conductance fluctuations are visible in the low-temperature conductance over a wide range of the gate voltages with an amplitude of the order of $0.01e^2/h$ that get smeared at higher temperatures. Unlike the longer segments, the short segments displayed a conductance of $(0.1–1)e^2/h$. The conductance fluctuations for the other samples (sample B and C) and for short probes are presented in the Supplemental Material [37].

We now proceed to discuss the multifractal analysis of the conductance fluctuations in the helical edge dominated transport regime. We employ the multifractal detrended fluctuation analysis (MF DFA) which identifies the deviations within a fictitious time period in fractal structure with large and small fluctuations. The gate voltage V_g or the charge density is considered as fictitious time. Therefore we analyze the dimensionless conductance $g_k = g(V_k) = G/(e^2/h) \ldots k = 1, 2 \ldots N$ series obtained by varying the gate voltage with fixed increment ΔV, where N is the total length of the series. Performing the first step we determine the profile

$$\tilde{g}(i) = \sum_{k=1}^{i} (g_k - \langle g \rangle), \tag{1}$$

where $\langle g \rangle$ is the zero mean profile of the original series g_k. The next step in the DFA procedure involves dividing the profile $\tilde{g}(i)$ into $M_s = \mathrm{int}(M/s)$ nonoverlapping segments of equal length s. The third step is the calculation of the local trend for each of the M_s segments by a least-square fit of the series. Therefore we determine the variance:

$$F_s^2(j) = \frac{1}{s} \sum_{k=1}^{i} \{\tilde{g}(i)[(j-1)s + i] - P_j(i)\}^2. \tag{2}$$

Here, $P_j(i)$ is the fitting polynomial over the jth segment of size s. Executing the fourth step we average over all segments to obtain the qth order fluctuation function:

$$F_q(s) = \left(\frac{1}{M_s} \sum_{j=1}^{M_s} [F_s^2(j)]^{q/2} \right)^{1/q}. \tag{3}$$

Finally in order to determine the scaling behavior of the fluctuation functions we analyze log-log plots of $F_q(s)$ versus s for each value of q. One would expect that $F_q(s)$ increases, for large values of s, as a power law: $F_q(s) \sim s^{H(q)}$, where $H(q)$ is the generalized Hurst exponent. For a monofractal series, $H(q)$ is independent of q, since the average over segment in in equation for $F(q)$ will give just this identical scaling behavior for all values of q. Another way to characterize a multifractal series is based on the determination of the width of the singularity spectrum $f(\alpha)$. Let us first define the parameter $\tau(q)$: $\tau(q) = qH(q) - 1$.

The singularity spectrum $f(\alpha)$ is related to $\tau(q)$ via a Legendre transform $f(\alpha) = \alpha q - \tau(q)$. Therefore the strength of the multifractal character of the fluctuations can be estimated from the width of $f(\alpha)$, $\Delta\alpha = \alpha_{\max} - \alpha_{\min}$. One would expect $f(\alpha)$ to have a shape of a wide symmetric arc for multiftactal spectrum, which becomes only a tiny arc with $\Delta\alpha \to 0$ when the spectrum involved begins to lose its multifractal nature.

Figure 3(a) shows representative plots of $\log[F_q(s)]$ versus $\log[s]$, from our data series for $G(V_g)$ shown in Fig. 2(a) for sample A; the circles represent the data points, and the solid lines are linear fits to the data for $q = \pm 4$. One can see that the scaling function $F_q(s)$ and corresponding regression slopes are q dependent. The difference between the q order for positive q = 4 and negative q = −4 are more distinct for smaller segment sizes s compared with the larger ones.

Figure 3(b) shows the mean Hurst exponent $H(q)$ from our data series for $G(V_g)$ shown in Fig. 2(a), as a function of the order q for different temperatures. One can see strong variation of $H(q)$ with q for all temperatures; however the interval of such variations becomes narrower at higher temperatures. Notice that the monofractal series have no periods with small and large fluctuations, and the Hurst exponent is expected to be q independent. Therefore our

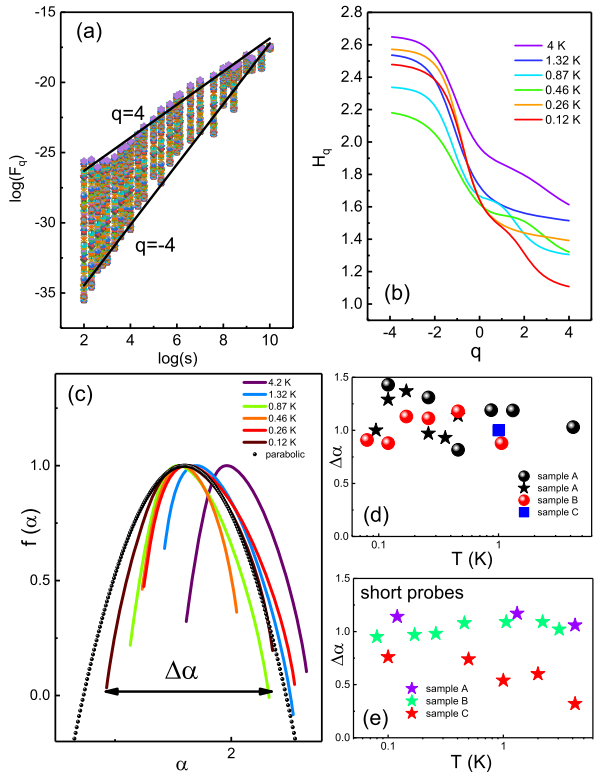

FIG. 3. The multifractality of the helical edge states' resistance fluctuations for sample A [Fig. 2(a)]. (a) The MF DFA fluctuation functions $F_q(s)$ are shown versus the scale s in log-log plots, T = 0.12 K. (b) The mean generalized Hurst exponent $H(q)$ of the resistance fluctuations for sample A. (c) The multifractal singularity spectrum of the resistance fluctuations for sample A. Dots-parabolic law with parameters given in the text. (d) The width of the multifractal spectrum as a function of T for both samples taken for different long segments: black circles, dataset in Fig. 1(a); black stars, Fig. 1(b); square, see dataset in the Supplemental Material [37] Fig. 2. (e) The width of the multifractal spectrum as a function of T for both samples taken for short segment 8–9 (see dataset in the Supplemental Material [37]).

analysis confirms that conductance fluctuations are multifractal, and that these features are stronger at lower temperatures.

In Fig. 3(c) we plot the mean multifractal spectrum $f(\alpha)$ as a function of the parameter α calculated from our data series for $G(V_g)$ for sample A and for different temperatures. One can see the spectrum with left truncations for several fixed values of T. These truncations originate from the leveling q order H_q exponent for positive $q's$ [Fig. 3(b)], because fluctuations have a multifractal structure that is insensitive to the local fluctuations with a large magnitude. In the Supplemental Material we present plots with $\log[F_q(s)]$, the mean Hurst exponent $H(q)$, and the spectrum $f(\alpha)$ from our data series for $G(V_g)$ for sample B [37]. Again our analysis confirms that the conductance fluctuations in sample B are multifractal. We should note the we analyzed singularity spectra $f(\alpha)$, corresponding to different voltage ranges [37]. We observe the persistence of multifractality across different gate voltage ranges. Finally in the Supplemental Material we provide justification of multifractality for different probe configuration for all three devices [37].

Figures 3(d) and 3(e) illustrate the width of the multifractal spectrum as a function of T for three samples for long and short segments. Notice that the width of the spectrum $\Delta\alpha$ at lower temperature is larger for sample A. One can see that while the amplitude of the oscillations shows significant temperature dependence, the uncertainties inherent in our experimental statistics hinder us from making conclusive statements regarding the temperature dependence of multifractality. As mentioned above, the average conductance of the short voltage probe is found to be close to the value of e^2/h, indicating quasiballistic transport. However, the transport of helical edge states demonstrates multifractal characteristics. Upon analyzing sample C, it becomes apparent that there is a decrease in $\Delta\alpha$ as the temperature rises. We suggest that although sample C possesses a similar quality to sample B, the local density of states for a short segment, which governs statistical fluctuations, might exhibit reduced disorder. At high temperature $T \sim 10$ K oscillations are smeared out and lose their multifractal nature (not shown). Note, that despite the strong variations in conductance, we did not find compelling evidence of a significant dependence of multifractality on the disorder level [37].

Now it would be instructive to put our observations in the context of Anderson localization transition. A nontrivial topology, as, e.g., in the integer quantum Hall effect and the quantum spin Hall effect, results in the Anderson transitions between distinct topological phases. One of the characteristic features of the Anderson transition are the mesoscopic conductance fluctuations, which relate to the local density of states or the nature of the electron wave function [39]. In the quantum Hall effect (QHE) the Chalker-Coddington network model serves as a standard model for studying the critical properties at the Anderson transition between different quantum Hall states [40]. A high-precision evaluation of the multifractal spectrum at the IQH transition has been performed in Ref. [28]. It has been shown that the multifractal $f(\alpha)$ spectrum is well described by a parabolic form. A multifractal spectrum has been observed recently in a single graphene layer confirming the validity of the Anderson localization model [34]. Moreover, a link between conductance fluctuation in the QHE regime and multifractal complex hierarchical phenomena in stochastic dynamics has been emphasized [35].

In quantum spin Hall effect or in 2D topological insulators with helical edge states the Anderson transition is expected to occur when the Fermi level crosses the bulk gap, where fluctuations of the potential are expected due

to the local random variations of the quantum well width. This results in a network of zero energy channels running along the boundaries separating the normal insulator and the 2D TI phases. In contrast to the quantum Hall states, the 2D TI-metal transition could be represented by uncoupled counterpropagating channels with opposite spin, the so-called Z_2 network model [41]. In gapless HgTe quantum wells with 6.3 nm width the total conductance is determined by a percolation along the zero-gap lines, when chemical potential crosses the charge neutrality point [42]. In a sample with 8.3 nm width the gap is large and transition is expected to occur, when chemical potential is close to the conduction or the valence band edges. Note, however, that our devices are strongly disordered with $G \ll e^2/h$. Secondly, the chemical potential does not vary linearly with the gate voltage, and a broad interval ΔV_g, in which the conductance fluctuations are observed, testifies to a large density of states in the band gap. In our samples we observed nonlocal effects which prove that the bulk of the samples remains insulating [6,22]. However, the electrons spend a significant amount of time diffusing randomly in the bulk away from the edge and forming a local network. Because of the helical nature of the channels the backscattering may occur near the sample edge in contrast to the QHE, where the network is chiral, and current should flow through the bulk.

Therefore the large mesoscopic fluctuations in our device can be attributed to an Anderson transition between localized and delocalized states similar to transitions between different quantum Hall states. Disordered average moment of the local density of states in quantum spin Hall states demonstrates power law scaling with a multifractal exponent [27,30,43]. According to numerical analysis performed in Ref. [43] the singularity spectrum $f(\alpha)$ has a parabolic form $f(\alpha) = 2 - (\alpha - \alpha_0)^2/[4(\alpha_0 - 2)]$, where $\alpha_0 = 2.125$. Figure 3(a) shows a fit to our data for $T = 0.12$ K and a parabola given by $2f(\alpha) = 2 - (\alpha - \alpha_0)^2/[2(\alpha_0 - 1.4)]$ with $\alpha_0 = 1.6$. Notice that the theoretical spectrum is predicted to be 2 times wider than we find in the experiment (multiple 2 is due to different definitions).The deviation from theory that we have observed may be attributed to the limitations of our experimental setup. Specifically, we are constrained by signal noise and the range of gate voltage within the gap.

In conclusion we observe a multifractality of the conductance fluctuation in a 2D topological insulator based on HgTe quantum well in the regime of the helical edge state transport. We attribute this effect to mesoscopic fluctuations of the local density of states, which are reflected in the conductance due to the strong coupling between the helical edge and bulk states. It would be interesting to explore the interplay between topology and interaction, which is expected for the spin quantum Hall symmetry class [30].

Discussions and correspondence with M. V. Entin, M. V. Feigel'man, and G. L. Vasconcelos are gratefully acknowledged. This work was supported by RSF Grant No. 23-22-00195.

[1] M. Z. Hasan and C. L. Kane, Colloquium: Topological insulators, Rev. Mod. Phys. **82**, 3045 (2010).
[2] X.-L. Qi and S.-C. Zhang, Topological insulators and superconductors, Rev. Mod. Phys. **83**, 1057 (2011).
[3] Y. Ren, Z. Qiao, and Q. Niu, Topological phases in two dimensional materials: A review, Rep. Prog. Phys. **79**, 066501 (2016).
[4] D. Culcer, A. C. Keser, Y. Li, and G. Tkachov, Transport in two-dimensional topological materials: Recent developments in experiment and theory, 2D Mater. **7**, 022007 (2020).
[5] M. Konig, S. Wiedmann, C. Brüne, A. Roth, H. Buhmann, L. W. Molenkamp, X.-L. Qi, and S.-C. Zhang, Quantum spin Hall insulator state in HgTe quantum wells, Science **318**, 766 (2007).
[6] G. M. Gusev, Z. D. Kvon, O. A. Shegai, N. N. Mikhailov, S. A. Dvoretsky, and J. C. Portal, Transport in disordered two-dimensional topological insulators, Phys. Rev. B **84**, 121302(R) (2011).
[7] E. B. Olshanetsky, Z. D. Kvon, G. M. Gusev, A. D. Levin, O. E. Raichev, N. N. Mikhailov, and S. A. Dvoretsky, Persistence of a Two-Dimensional Topological Insulator State in Wide HgTe Quantum Wells, Phys. Rev. Lett. **114**, 126802 (2015).
[8] Chen-Hsuan Hsu, Peter Stano, Jelena Klinovaja, and Daniel Loss, Helical liquids in semiconductors, Semicond. Sci. Technol. **36**, 123003 (2021).
[9] Oleg M. Yevtushenko and Vladimir I. Yudson, Protection of edge transport in quantum spin Hall samples: Spin-symmetry based general approach and examples, New J. Phys. **24**, 023040 (2022).
[10] G. M. Gusev, Z. D. Kvon, E. B. Olshanetsky, and N. N. Mikhailov, Mesoscopic transport in two-dimensional topological insulators, Solid State Commun. **302**, 113701 (2019).
[11] J. Maciejko, C. Liu, Y. Oreg, X. L. Qi, C. Wu, and S. C. Zhang, Kondo Effect in the Helical Edge Liquid of the Quantum Spin Hall State, Phys. Rev. Lett. **102**, 256803 (2009).
[12] B. L. Altshuler, I. L. Aleiner, and V. I. Yudson, Localization at the Edge of a 2D Topological Insulator by Kondo Impurities with Random Anisotropies, Phys. Rev. Lett. **111**, 086401 (2013).
[13] O. M. Yevtushenko and V. I. Yudson, Kondo Impurities Coupled to a Helical Luttinger Liquid: RKKY-Kondo Physics Revisited, Phys. Rev. Lett. **120**, 147201 (2018).
[14] C.-H. Hsu, P. Stano, J. Klinovaja, and D. Loss, Effects of nuclear spins on the transport properties of the edge of two-dimensional topological insulators, Phys. Rev. B **97**, 125432 (2018).
[15] T. I. Schmidt, S. Rachel, F. von Oppen, and L. I. Glazman, Inelastic Electron Backscattering in a Generic Helical Edge Channel, Phys. Rev. Lett. **108**, 156402 (2012).

[16] N. Kainaris, I. V. Gornyi, S. T. Carr, and A. D. Mirlin, Conductivity of a generic helical liquid, Phys. Rev. B **90**, 075118 (2014).
[17] J. I. Väyrynen, D. I. Pikulin, and J. Alicea, Noise-Induced Backscattering in a Quantum Spin Hall Edge, Phys. Rev. Lett. **121**, 106601 (2018).
[18] J. C. Budich, F. Dolcini, P. Recher, and B. Trauzettel, Phonon-Induced Backscattering in Helical Edge States, Phys. Rev. Lett. **108**, 086602 (2012).
[19] A. Ström, H. Johannesson, and G. I. Japaridze, Edge Dynamics in a Quantum Spin Hall State: Effects from Rashba Spin-Orbit Interaction, Phys. Rev. Lett. **104**, 256804 (2010).
[20] J. I. Väyrynen, M. Goldstein, and L. I. Glazman, Helical Edge Resistance Introduced by Charge Puddles, Phys. Rev. Lett. **110**, 216402 (2013).
[21] J. I. Väyrynen, M. Goldstein, Y. Gefen, and L. I. Glazman, Resistance of helical edges formed in a semiconductor heterostructure, Phys. Rev. B **90**, 115309 (2014).
[22] G. M. Gusev, Z. D. Kvon, E. B. Olshanetsky, A. D. Levin, Y. Krupko, J. C. Portal, N. N. Mikhailov, and S. A. Dvoretsky, Temperature dependence of the resistance of a two-dimensional topological insulator in a HgTe quantum well, Phys. Rev. B **89**, 125305 (2014).
[23] G. Grabecki, J. Wróbel, M. Czapkiewicz, L. Cywiński, S. Gieraltowska, E. Guziewicz, M. Zholudev, V. Gavrilenko, N. N. Mikhailov, S. A. Dvoretski, F. Teppe, W. Knap, and T. Dietl, Nonlocal resistance and its fluctuations in microstructures of band-inverted HgTe/(Hg,Cd)Te quantum wells, Phys. Rev. B **88**, 165309 (2013).
[24] Kalle Bendias, Saquib Shamim, Oliver Herrmann, Andreas Budewitz, Pragya Shekhar, Philipp Leubner, Johannes Kleinlein, Erwann Bocquillon, Hartmut Buhmann, and Laurens W. Molenkamp, High mobility HgTe microstructures for quantum spin Hall studies, Nano Lett. **18**, 4831 (2018).
[25] A. V. Bubis, N. N. Mikhailov, S. A. Dvoretsky, A. G. Nasibulin, and E. S. Tikhonov, Localization of helical edge states in the absence of external magnetic field, Phys. Rev. B **104**, 195405 (2021).
[26] Vadim Cheianov and Leonid I. Glazman, Mesoscopic Fluctuations of Conductance of a Helical Edge Contaminated by Magnetic Impurities, Phys. Rev. Lett. **110**, 206803 (2013).
[27] F. Evers and A. D. Mirlin, Anderson transitions, Rev. Mod. Phys. **80**, 1355 (2008).
[28] F. Evers, A. Mildenberger, and A. D. Mirlin, Multifractality of wave functions at the quantum Hall transition revisited, Phys. Rev. B **64**, 241303(R) (2001).
[29] Anderson L. R. Barbosa, Tiago H. V. de Lima, Iván R. R. González, Nathan L. Pessoa, Antônio M. S. Macêdo, and Giovani L. Vasconcelos, Turbulence Hierarchy and Multifractality in the Integer Quantum Hall Transition, Phys. Rev. Lett. **128**, 236803 (2022).
[30] S. S. Babkin and I. S. Burmistrov, Generalized multifractality in the spin quantum Hall symmetry class with interaction, Phys. Rev. B **106**, 125424 (2022).
[31] B. Sacepe, C. Chapelier, T. I. Baturina, V. M. Vinokur, M. R. Baklanov, and M. Sanquer, Disorder-Induced Inhomogeneities of the Superconducting State Close to the Superconductor-Insulator Transition, Phys. Rev. Lett. **101**, 157006 (2008).
[32] Kun Zhao *et al.*, Disorder-induced multifractal superconductivity in monolayer niobium dichalcogenides, Nat. Phys. **15**, 904 (2019).
[33] P. A. Lee, A. D. Stone, and H. Fukuyama, Universal conductance fluctuations in metals: Effects of finite temperature, interactions, and magnetic field, Phys. Rev. B **35**, 1039 (1987).
[34] K. R. Amin, S. S. Ray, N. Pal, R. Pandit, and A. Bid, Exotic multifractal conductance fluctuations in graphene, Commun. Phys. **1**, 1 (2018).
[35] N. L. Pessoa, A. L. R. Barbosa, G. L. Vasconcelos, and A. M. S. Macedo, Multifractal magnetoconductance fluctuations in mesoscopic systems, Phys. Rev. E **104**, 054129 (2021).
[36] Kazi Rafsanjani Amin, Ramya Nagarajan, Rahul Pandit, and Aveek Bid, Multifractal Conductance Fluctuations in High-Mobility Graphene in the Integer Quantum Hall Regime, Phys. Rev. Lett. **129**, 186802 (2022).
[37] See Supplemental Material at http://link.aps.org/supplemental/10.1103/PhysRevLett.131.076301 for samples *A*, *B*, and *C*, as well as the analysis of their multifractality.
[38] N. N. Mikhailov, R. N. Smirnov, S. A. Dvoretsky, Yu. G. Sidorov, V. A. Shvets, E. V. Spesivtsev, and S. V. Rykhlitski, Growth of $Hg_{1-x}Cd_xTe$ nanostructures by molecular beam epitaxy with ellipsometric control, Int. J. Nanotechnology **3**, 120 (2006).
[39] I. V. Lerner, Distribution functions of current density and local density of states in disordered quantum conductors, Phys. Lett. A **133**, 253 (1988).
[40] J. T. Chalker and P. D. Coddington, Percolation, quantum tunnelling and the integer Hall effect, J. Phys. C **21**, 2665 (1988).
[41] M. Onoda, Y. Avishai, and N. Nagaosa, Localization in a Quantum Spin Hall System, Phys. Rev. Lett. **98**, 076802 (2007).
[42] G. M. Gusev, Z. D. Kvon, D. A. Kozlov, E. B. Olshanetsky, M. V. Entin, and N. N. Mikhailov, Transport through the network of topological channels in HgTe based quantum well, 2D Mater. **9**, 015021 (2022).
[43] F. Evers, A. Mildenberger, and A. D. Mirlin, Multifractality at the spin quantum Hall transition, Phys. Rev. B **67**, 041303(R) (2003).